

1 **The higher relative concentration of K⁺ to Na⁺ in saline**
2 **water improves soil hydraulic conductivity, salt leaching**
3 **efficiency and structural stability**

4 Sihui Yan ^{a, b}, [Tibin Zhang](#) ^{a, c, *}, Binbin Zhang ^{a, b}, Tonggang Zhang ^{a, b}, Yu Cheng ^{a, b},
5 Chun Wang ^{a, b}, Min Luo ^{a, b}, Hao Feng ^{a, c}, Kadambot H.M. Siddique ^d

6 ^a. Key Laboratory of Agricultural Soil and Water Engineering in Arid and Semiarid
7 Areas, Ministry of Education, Northwest A&F University, Yangling, Shaanxi 712100,
8 P. R. China

9 ^b. College of Water Resources and Architecture Engineering, Northwest A&F
10 University, Yangling, Shaanxi 712100, P. R. China

11 ^c. Institute of Soil and Water Conservation, Northwest A&F University, Yangling,
12 Shaanxi 712100, P. R. China

13 ^d The UWA Institute of Agriculture, The University of Western Australia, Perth, WA
14 6001, Australia

15 * Corresponding author at: Institute of Soil and Water Conservation, Northwest A&F
16 University, Yangling, Shaanxi 712100, China. Tel.: +86 29 87012871; fax: +86 29
17 87011354. E-mail: zhangtibin@163.com (T. Zhang)

18 **Abstract**

19 Soil salinity and sodicity caused by saline water irrigation are widely observed
20 globally. Clay dispersion and swelling are influenced by sodium (Na^+) concentration
21 and electrical conductivity (EC) of soil solution. Specifically, soil potassium (K^+) also
22 significantly affects soil structural stability, but which concern was rarely addressed in
23 previous studies or irrigation practices. A soil column experiment was carried out to
24 examine the effects of saline water with different relative concentrations of K^+ to Na^+
25 (K^+/Na^+), including K^+/Na^+ of 0:1 (K0Na1), 1:1 (K1Na1), 1:0 (K1Na0) at a constant
26 EC (4 dS m^{-1}), and deionized water as the control (CK), on soil physicochemical
27 properties. The results indicated that at the constant EC of 4 dS m^{-1} , the infiltration rate
28 and water content were significantly ($P < 0.05$) affected by K^+/Na^+ values, K0Na1,
29 K1Na1 and K1Na0 significantly ($P < 0.05$) reduced saturated hydraulic conductivity by
30 43.62%, 29.04% and 18.06% respectively compared with CK. The volumetric water
31 content was significantly ($P < 0.05$) higher in K0Na1 than CK at both 15 and 30 cm soil
32 depths. K1Na1 and K1Na0 significantly ($P < 0.05$) reduced the desalination time and
33 required leaching volume. K0Na1 and K1Na1 reached the desalination standard after
34 the fifth and second infiltration, respectively, as K1Na0 did not exceed the bulk
35 electrical conductivity required for desalination prerequisite throughout the whole
36 infiltration cycle at 15 cm soil layer. Furthermore, due to the transformation of
37 macropores into micropores spurred by clay dispersion, soil total porosity in K0Na1
38 dramatically decreased compared with CK, and K1Na0 even increased the proportion

删除了: +,

40 of soil macropores. The higher relative concentration of K^+ to Na^+ in [saline](#) water was
41 more conducive to soil aggregates stability, alleviating the risk of macropores reduction
42 caused by sodicity.

43 **Keywords:** Saline water; Cation composition; Hydraulic properties; Desalination; Pore
44 structure.

45 1 Introduction

46 Freshwater shortage resulted from elevated demand for water resources as well as
47 the irrational exploitation and use after economic and population growth (Zhang and
48 Xie 2019; Prajapati et al. 2021), constrains the sustainability of agricultural production
49 (Aparicio et al., 2019). Alternative water resources with variable water quality (such as
50 saline water) are being considered for agricultural irrigation in several desert and saline
51 areas (Singh et al. 2021; Liu et al. 2022a). Utilizing saline water could partly alleviate
52 the undersupply of freshwater for agricultural production (Yang et al., 2020). However,
53 the other side of the coin is that saline water irrigation could result in soil salinization
54 and/or sodicity. [Once the soil is salinized and/or alkalized, soil hydraulic properties,](#)
55 [like infiltration rate, saturated hydraulic conductivity and permeability, will change](#)
56 [inevitably \(Scudiero et al., 2017\). And cations in the soil solution change the soil](#)
57 [structural characteristics through the soil clay particle dispersion and flocculation](#)
58 [\(Bouksila et al. 2013; Hack-ten Broeke et al. 2016; Zhang et al. 2018\).](#) Therefore, in
59 order to optimize saline water utilization, the effects of saline water quality on the soil

删除了: applied

删除了: This disaster is related directly to soil pore size distribution, and in turn to the dispersion and swelling of the clay fraction (Bouksila et al.

64 hydraulic properties and pore structure characteristics should be paid more attention.

删除了: (Scudiero et al., 2017).

65 Saline water irrigation can increase the monovalent ions concentration in soil

66 solution and affect soil structure (Qadir et al. 2007; Qadir et al. 2021). Excess sodium

67 (Na^+) from saline irrigation water is adsorbed onto the clay surface in salt-affected soils

删除了: saline

68 where sodium compounds predominate contributing to the disintegration of soil

删除了: exchange

69 structure (Marchuk and Rengasamy 2011; Belkheiri and Mulas 2013; Awadat et al.

70 2021). As percolation progresses, the thickness of the diffusion double electron layers

71 increases due to the relatively larger hydrated radius of Na^+ , and the repulsive force

删除了: raises

72 between adjacent diffusion double electron layers appears to increase, resulting in the

73 dispersion and swelling of soil particles (Alva et al. 1991; Reading et al. 2015).

74 Soil calcium (Ca^{2+}) and magnesium (Mg^{2+}) can alleviate soil dispersibility by

75 replacing Na^+ in soil colloids, the outer layers of the Ca^{2+} and Mg^{2+} containing colloidal

删除了: layer

76 particles do not adsorb water molecules, turning Na^+ qualitative hydrophilic colloid into

77 Ca^{2+} and Mg^{2+} hydrophobic colloids (Marchuk and Rengasamy 2011; Tsai et al. 2012).

删除了: colloid

78 Colloidal particles move closer to each other, promoting soil particles forming water

删除了: get close

79 stable aggregates, thus improving soil structural stability (Gharaibeh et al. 2009;

80 McKenna et al. 2019). Therefore, the concentration of Na^+ in relation to Mg^{2+} and Ca^{2+}

81 (sodium adsorption ratio, SAR) (U.S. Salinity Laboratory Staff 1954) is a crucial

删除了: Sodium

82 criterion for soil structural stability and hydraulic conductivity (Rengasamy and

删除了: considered

83 Marchuk 2011). Although SAR can be used to predict soil clay dispersion effect caused

删除了: in

84 by cations, the controlling mechanism of dispersion in SAR is presumed to be

95 exchangeable Na^+ . However, Na^+ does not alone cause soil dispersion since the
96 chemical component of clay structure integrity is mainly a function of ionic valence
97 and hydration radius (Marchuk et al., 2014). Potassium (K^+) has been overlooked
98 because salt-affected soils typically contain low amounts of K^+ . However, Li et al.
99 (2022) reported that under the continuous recycling use of underground saline water,
100 water-soluble and exchangeable K^+ is higher than Ca^{2+} and Mg^{2+} in the Hetao irrigation
101 district—one of the large irrigation districts in China. It is anticipated that the long-term
102 use of irrigation water with high K^+ concentrations may therefore create substantial
103 challenges in preserving good soil structure and adequate infiltration rates (Sposito et
104 al., 2016). K^+ is not as effective as Na^+ in generating soil particle dispersion and
105 swelling problems, yet Marchuk and Marchuk (2018) pointed out that K^+ could
106 substitute Na^+ on exchange sites to encourage Na^+ leaching and increase water
107 conductivity to some extent. A lower concentration of K^+ may have positive effects on
108 soil permeability due to the substitution of exchangeable Na^+ by K^+ with lower
109 dispersive potential, increasing aggregates stability and soil pore connectivity (Buelow
110 et al., 2015). [Traditional SAR ignored the role of \$\text{K}^+\$, a newly proposed equation, cation](#)
111 [ratio of soil structural stability \(CROSS\) could integrate the effects of \$\text{Na}^+\$ and \$\text{K}^+\$ in](#)
112 [soil, which is an important indicator for assessing the quality of saline water](#)
113 [\(Rengasamy and Marchuk 2011\).](#)

114 Thus, we hypothesized that the amount of K^+ relative to Na^+ would certainly have
115 an effect on soil structural stability, [which could be evaluated in](#) a column experiment

删除了: and these relationships

删除了: well

删除了: by

119 under controlled conditions. The specific objectives of this study were to (1) ascertain
120 the effect of irrigation saline water with different relative concentrations of K^+ to Na^+
121 (K^+/Na^+) on transport and distribution of water and salt; (2) determine the effect on soil
122 pore structural characteristics; (3) predict these effects using a newly proposed index
123 (CROSS) rather than SAR.

124 2 Materials and methods

125 2.1 Soil sampling location and properties

126 The study soil was collected from a layer of 0–40 cm field in Yangling (108°04'E,
127 34°20'N), Shaanxi Province, China. After air-dried, the soil was grounded to pass
128 through a 2-mm sieve. Soil's physical and chemical properties are listed in Table 1. Soil
129 particle size distribution was measured by the Laser Mastersizer 2000 (Malvern
130 Instruments, Malvern, UK), and according to the [international](#) classification system,
131 soil texture [was](#) classified as silty clay. Soil bulk density [was](#) calculated [using the soil](#)
132 [core method](#). EC_e and pH were measured [using](#) conductivity meter (DDS-307, China)
133 and pH meter (PHS-3C, China), respectively. [Total soluble salts refer to the total](#)
134 [amount of soluble salts in soil-saturated paste extract](#). Flame photometry (6400A, China)
135 was used to measure soluble Na^+ and K^+ , [concentrations of](#) CO_3^{2-} and HCO_3^- were
136 tested [using](#) the neutral titration method, Cl^- was analyzed [using](#) the silver nitrate
137 titration method, and SO_4^{2-} was determined [using](#) barium sulfate turbidimetric method,
138 Mg^{2+} and Ca^{2+} were specified using ethylene diamine tetraacetic acid (EDTA)

删除了: -

删除了: USDA

删除了: is

删除了: loam

删除了: by

删除了: was 1.35 g cm⁻³. The soil had a low salt concentration with EC_e (electrical conductivity of saturated extract) of 0.72 dS m⁻¹ and pH of 7.66, respectively.

删除了: by

设置了格式

删除了: concentrations

删除了: by

删除了: by

删除了: by

152 titrimetric method (Bao 2005).

153 Table 1 The physicochemical properties of study soil.

Property	Value
Particle size distribution (%)	
Sand (> 0.05 mm)	8.10
Silt (0.05-0.002 mm)	60.62
Clay (<0.002 mm)	31.28
Texture	Silty clay
EC _e (dS m ⁻¹)	0.72
pH	7.66
<u>Total soluble salts (g Kg⁻¹)</u>	<u>0.14</u>
Ion concentration (mmol L ⁻¹)	
CO ₃ ²⁻ +HCO ₃ ⁻	0.60
Cl ⁻	0.23
SO ₄ ²⁻	2.18
Mg ²⁺	0.32
Ca ²⁺	0.54
Na ⁺	0.10
K ⁺	< 0.01

154 Note: EC_e is electrical conductivity of soil-saturated extract.

155 2.2 Experimental design

156 Soil columns were prepared using transparent polyvinyl chloride cylinders, with
157 an internal diameter of 20 cm and a height of 50 cm (Fig. 1). Round and small holes (6
158 mm diameter) were arranged equally at the bottom of each cylinder for drainage. A 5
159 cm depth quartz sand was laid at the bottom of the soil column as a filter layer before
160 packing to prevent small soil particles from being washed away. After that, air-dried
161 soil was packed at 40 cm height with a bulk density of 1.35 g cm⁻³ (referring to the
162 original level of the soil). The sieved dry soil was poured into each soil column in the

删除了:

格式化表格

删除了:-

删除了: loam

格式化表格

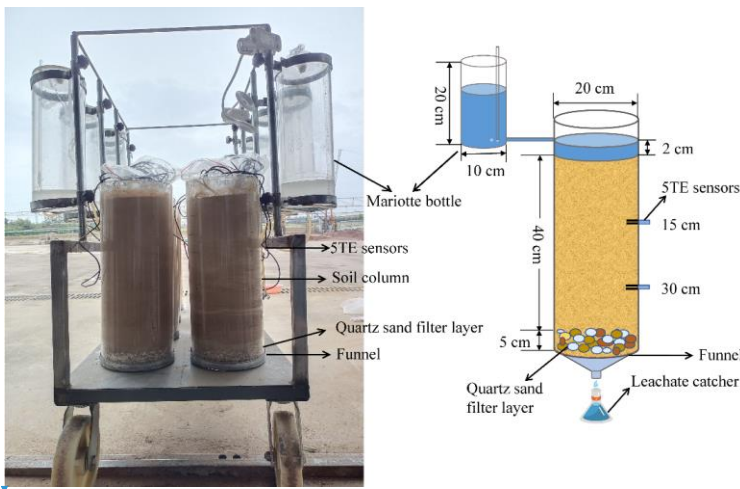
删除了: represents

删除了:

删除了: Experiment

删除了: equally

173 5-cm sections for uniform compaction, and the layer's surface was roughened to ensure
 174 a tight connection to the next layer. The soil column was then allowed to stand in the
 175 laboratory for 24 hours before [starting](#) the experiments described herein. The constant
 176 water head (2 cm, using a Mariotte bottle) infiltration experiment was conducted with
 177 [3](#) replications for each treatment.



178
 179 Fig. 1. Illustration of the experiment apparatus (a) and schematic diagram (b).

180 Three infiltration solutions were prepared with different ratios of K^+/Na^+ [(0:1
 181 (K0Na1), 1:1 (K1Na1), 1:0 (K1Na0)] at constant EC of 4 dS m^{-1} , [with](#) deionized water
 182 [was used](#) as the control (CK) (Table 2). The cation ratio of soil structural stability
 183 (CROSS) (Rengasamy and Marchuk 2011) [is](#) an indicator of soil structural behavior as
 184 influenced by both Na^+ and K^+ , and it was calculated [as follows](#) (Smith et al., 2015):

$$CROSS = \frac{Na^+ + 0.335K^+}{[(Ca^{2+} + 0.0758Mg^{2+})/2]^{0.5}} \quad (1)$$

186 where [the](#) chemical element symbols denote charge concentrations ($\text{mmol}_c \text{ L}^{-1}$).

删除了: the initiation of

删除了: three



删除了:

删除了: (

删除了:)

删除了: and

删除了: was

删除了: accordingly

删除了: different

196 Table 2 Saline water settings with different K⁺/Na⁺ at a constant EC.

Treatment	Added salt/ (mmol L ⁻¹)			K ⁺ /Na ⁺	Setting	Measured	CROSS (mmol _c L ⁻¹) ^{0.5}
	KCl	NaCl	CaCl ₂		EC (dS m ⁻¹)	EC (dS m ⁻¹)	
K0Na1	0	34	3	0:1	4.00	4.25	27.76
K1Na1	17	17	3	1:1	4.00	4.33	17.49
K1Na0	34	0	3	1:0	4.00	4.40	7.22
CK	Deionized water			/	0.00	0.02	/

197 Note: K0Na1, K1Na1 and K1Na0 indicate the saline water at EC of 4 dS m⁻¹ with
 198 K⁺/Na⁺ of 0:1, 1:1 and 1:0, respectively; CK, deionized water; CROSS represents cation
 199 ratio of soil structural stability.

200 The experiment implemented alternate leaching, as the prolonged leaching process
 201 of soil substrates is more helpful in illuminating the function of electrolyte effect and
 202 cation exchange (Shaygan et al., 2017). The next infiltration was performed two days
 203 after the drainage of the previous infiltration was completed. Soil layers were regarded
 204 as reaching desalination prerequisite when the soil salt content came to less than 0.3%,
 205 which meant that bulk electrical conductivity was less than 1.5 dS m⁻¹ (transformation
 206 from salt content to bulk electrical conductivity) (Yin et al., 2022). Water application
 207 was stopped when the bulk electrical conductivity of all treatments at 15 cm depth
 208 reached the prerequisite for desalination. This experiment was planned to fill all the
 209 pores in the soil column throughout the infiltration cycle, therefore the water applied at
 210 the first infiltration was described by the pore volume equation (Xu and Huang 2010):

$$V_p = V_s \cdot TP \quad (2)$$

$$TP = \frac{ds - BD}{ds} \quad (3)$$

213 where V_p is the pore volume (cm³), V_s is the volume of filled soil (cm³), TP is the soil

删除了:

删除了: Adding

删除了: was

删除了: in the form of

删除了: proved

删除了: useful for

220 total porosity (%), d_s is the soil particle density (2.65 g cm^{-3}) (Xu and Huang 2010),
221 BD is the bulk density (g cm^{-3}). According to Eq. (2) and Eq. (3), around 6 L of water
222 was required in the first infiltration. Required water volume for each subsequent
223 leaching was determined by the volume of leachate at the first infiltration, 0.5 L each
224 time.

225 2.3 [Soil properties measurements](#)

226 During the whole [experimental](#) period, soil volumetric water content and bulk
227 electrical conductivity were real-time monitored at 15 and 30 cm soil depths from the
228 soil surface by capacitance sensors (ECH2O 5TE, METER Group, USA) (Fig. 1).

229 [Leachate](#) was collected in the leachate catcher below the soil column. Cumulative
230 leachate volume was monitored over time to determine the saturated hydraulic
231 conductivity (K_{sat} , cm min^{-1}) of each treatment by using a derivation of Darcy's
232 approach (Sahin et al., 2011):

$$233 K_{\text{sat}} = \frac{V_1 \cdot H}{A \cdot t \cdot (H + h)} \quad (4)$$

234 where V_1 is the leachate volume (cm^3), H is the length of filled soil (cm), A is the surface
235 area of soil column (cm^2), t is the leaching time of measurement (min), h is the height
236 of constant water head (cm).

237 [To determine the amount of salt released, we measured the volume and EC of the](#)
238 [leachate. The leachate was collected at 3 h intervals when the leachate started to drain,](#)
239 [and leachate was stored in 100 ml wide-mouth polypropylene reagent bottles.](#) The salt

删除了: Measurements

删除了: experiment

删除了: The leachate

243 accumulated in the soil column was determined by subtracting the salt in the leachate
244 from the applied water, the salination rate (Rs , %) indicated the ratio of salt accumulated
245 in the soil column at every time of infiltration to the salt content at the first applied
246 water. Leaching efficiency (Le , g L^{-1}) [refers](#) to the amount of desalination per unit of
247 water volume in the desalination process. Rs and Le were calculated as follows:

$$248 \quad Rs = m_s / m_w \quad (5)$$

$$249 \quad Le = (m_s - m_1) / w \quad (6)$$

250 Where m_s is the salt content accumulated in soil column at [each](#) infiltration (g), m_w is
251 the salt content in the total water used for the first infiltration (g), m_1 is the mass of salts
252 after the first infiltration (g), w is the total water volume used for leaching (L).

253 Soil samples were collected from each soil column at 5-cm intervals with the 0-
254 40 cm soil layer three days after the final infiltration. Soil BD was calculated using the
255 soil core method, and TP was calculated by Eq. (3) based on BD . Soil water
256 characteristics curve was measured with the high velocity centrifugal method (CR21
257 Hitachi, Japan), and calibrated by RETC software (PC Progress Inc., Prague, Czech
258 Republic). Currently, several defining sizes of macropores are proposed, rather than a
259 precise definition and pore size range (Cameira et al. 2003; Kim et al. 2010; Hu et al.
260 2018; Budhathoki et al. 2022; Aldaz-Lusarreta et al. 2022). In this study, macropores
261 were defined as the pores with diameters larger than 1 mm, whereas micropores were
262 defined as smaller than 1 mm (Luxmoore 1981; Wilson and Luxmoore 1988). Based on
263 the capillary pressure data, the relationship between pore diameter (d , mm) and water

删除了: referred

删除了: every time of

删除了: -

267 suction (S , Pa) was described according to the capillary bundle model (Jury et al., 1991):

268
$$d = \frac{300}{S} \quad (7)$$

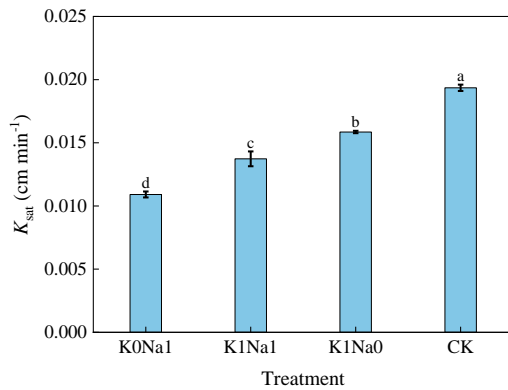
269 **2.4 Statistical analysis**

270 Statistical analysis among all treatments with different K^+/Na^+ was performed in
271 SPSS 22.0 software, using one-way analysis of variance (ANOVA) based on the least
272 significant difference (LSD) test at 95% significance level ($P < 0.05$). All figures were
273 created through Origin 2022b.

274 **3 Results**

275 **3.1 Soil saturated hydraulic conductivity (K_{sat})**

276 The K0Na1, K1Na1 and K1Na0 significantly ($P < 0.05$) reduced K_{sat} by 43.62%,
277 29.04% and 18.06% compared with CK, respectively (Fig. 2). Additionally, K_{sat} was
278 negatively correlated with CROSS of saline water, increasing the CROSS of the applied
279 saline water generally reduced K_{sat} . _____



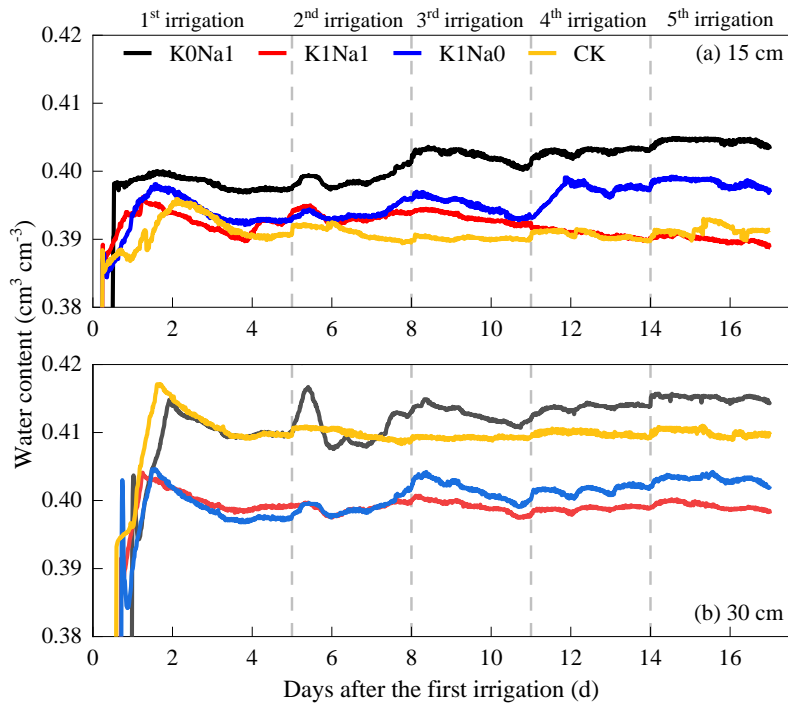
删除了:

280
 281 Fig. 2. Saturated hydraulic conductivity (K_{sat}) under different treatments. K0Na1,
 282 K1Na1 and K1Na0 indicate the saline water at EC of 4 dS m⁻¹ with K⁺/Na⁺ of 0:1, 1:1
 283 and 1:0, respectively; CK, deionized water; Different letters after means of K_{sat} indicate
 284 statistical differences ($P < 0.05$) among treatments based on LSD. Bars indicate
 285 standard deviations of means.

286 **3.2 Soil water content**

287 Water content increased immediately after each infiltration in all treatments, then
 288 gradually decreases and the degree of variation tends to stabilize (Fig. 3). And water
 289 content at deeper soil depths was greater than at shallow soil depths at the same time
 290 during the whole infiltration period. The water content ranged from 0.39-0.41 and
 291 0.40-0.42 cm³ cm⁻³ at 15 and 30 cm soil depths, respectively. K0Na1 had the highest
 292 water content at both 15 and 30 cm soil depths. K1Na1 and K1Na0 were greater than
 293 CK at 15 cm soil depth and lower than CK at 30 cm soil depth, and the water content
 294 of K1Na1 was higher than K1Na0 at both 15 and 30 cm soil layers.

删除了: for
 删除了: and
 删除了: declined
 删除了: a constant level
 删除了: -
 删除了: -
 删除了: gained



305

306 Fig. 3. Variation of water content over time under different treatments at 15 (a) and 30

307 cm (b) soil depths during the five times of infiltration.

308 3.3 Soil salination rate (R_s) and leaching efficiency (Le)

309 The R_s and Le under CK were not shown in Fig. 4, because deionized water was

310 used as the control and there was almost no salt contained in the study soil, CK was

311 considered negligible for salt accumulation and leaching. R_s peaked at the first

312 infiltration, and approximately 70%–80% of the salt in the saline water was retained in

313 the soil column, after which the subsequent leaching had lower R_s values (Fig. 4). The

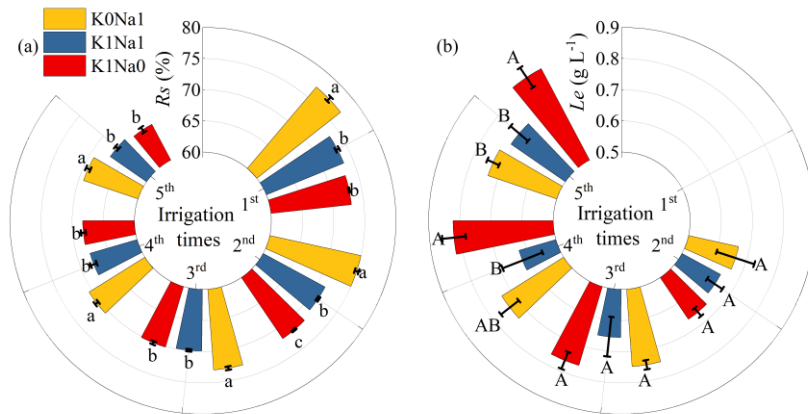
314 lower the relative concentration of K^+ to Na^+ , the larger soil R_s . Among the three saline

删除了: %-

删除了: ratio

删除了: +/

318 water treatments, K1Na0 had the lowest R_s and highest Le at five infiltrations.



319
320 Fig. 4. Salination rate (R_s) (a) and leaching efficiency (Le) (b) at five infiltrations under
321 all saline water treatments. K0Na1, K1Na1 and K1Na0 indicate the saline water at EC
322 of 4 dS m⁻¹ with K⁺/Na⁺ of 0:1, 1:1 and 1:0, respectively; Different lowercase letters
323 followed means of R_s indicate statistical differences ($P < 0.05$) among treatments based
324 on LSD, and different uppercase letters followed means of Le indicate statistical
325 differences ($P < 0.05$) among treatments based on LSD. Bars indicate standard
326 deviations of means.

327 3.4 Soil bulk electrical conductivity

328 Bulk electrical conductivity of K0Na1, K1Na1 and K1Na0 ranged from 1.0–2.0
329 dS m⁻¹ at 15 cm, 1.5–2.5 dS m⁻¹ at 30 cm soil depth (Fig. 5). After the first infiltration,
330 bulk electrical conductivity in 15 cm soil depth peaked, and then exhibited a general
331 downward trend in the following infiltrations. However, more salts were leached to

删除了: capital

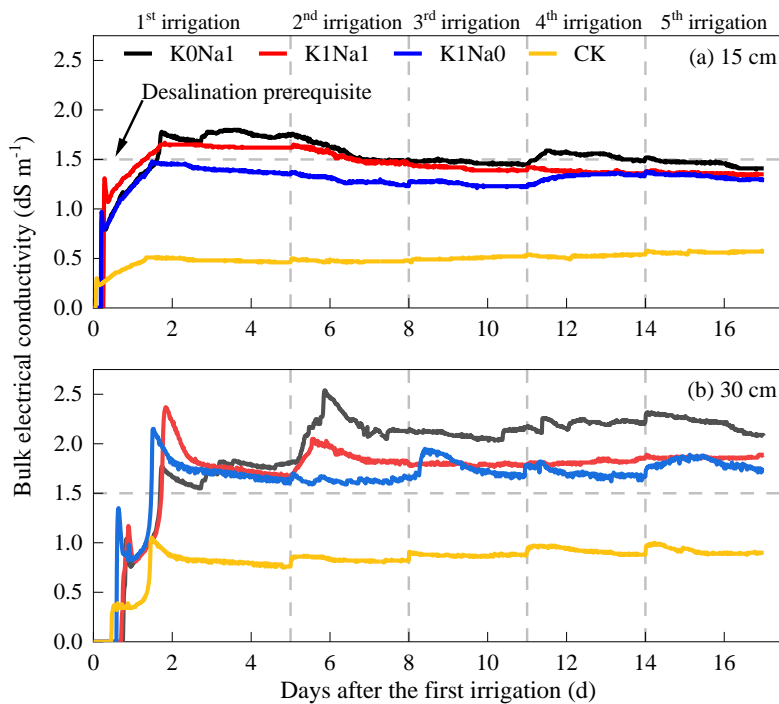
删除了: to

删除了: to

删除了: layer reached its apes

336 deeper layers, where salt began to accumulate instead of desalination, and bulk
 337 electrical conductivity at 30 cm soil depth gradually increased following the infiltration
 338 events. Overall, K0Na1 had the highest bulk electrical conductivity among all
 339 treatments at both 15 and 30 cm, and K1Na1 was quite higher than K1Na0.

删除了: At both 15 and 30 cm soil layers,
 删除了: of K0Na1 was considerably greater than K1Na1



340
 341 Fig. 5. Variation of bulk electrical conductivity over time under treatments with
 342 different K^+/Na^+ at constant EC at 15 (a) and 30 cm (b) soil depths in the period of five
 343 times of infiltration. K0Na1, K1Na1 and K1Na0 indicate the saline water at EC of 4 dS
 344 m^{-1} with K^+/Na^+ of 0:1, 1:1 and 1:0, respectively; CK, deionized water.

345 At 15 cm soil depth, K0Na1 reached the soil desalination prerequisite after the
 346 fifth infiltration, while K1Na1 reached the desalination prerequisite after the second
 347 infiltration, and K1Na0 did not exceed desalination prerequisite during the whole

350 infiltration period. Among all saline water treatments, K1Na0 reduced the desalination
351 time and required leaching volume to reach the standard of desalination. K0Na1,
352 K1Na1 and K1Na0 did not meet the desalination prerequisite at 30 cm soil depth, and
353 the increased volume of infiltration water also increased the bulk electrical conductivity.

删除了: saved

354 3.5 Soil bulk density (*BD*) and total porosity (*TP*)

355 Soil *BD* varied from 1.30–1.40 g cm⁻³ across all treatments, and *BD* was below
356 1.35 g cm⁻³ at 0–10 and 35–40 cm soil layers, however, over 1.35 g cm⁻³ at 10–35 cm
357 soil depth (Fig. 6). K0Na1 significantly ($P < 0.05$) enhanced soil *BD* throughout the soil
358 column profile compared with CK. *TP* first diminished with soil depth to reach a
359 minimum at about 30–35 cm, and then slightly increased at 35–40 cm. The *TP* of
360 K1Na1 and K1Na0 slightly improved after five times of infiltration, and only K0Na1
361 showed a decline compared with CK. Overall, over the whole infiltration period,
362 K1Na0 was most conducive to the formation of soil pore structure and increasing the
363 total pore volume. The saline water with lower CROSS was beneficial for reducing soil
364 *BD* and increasing *TP*.

删除了: between

删除了: and

删除了: for

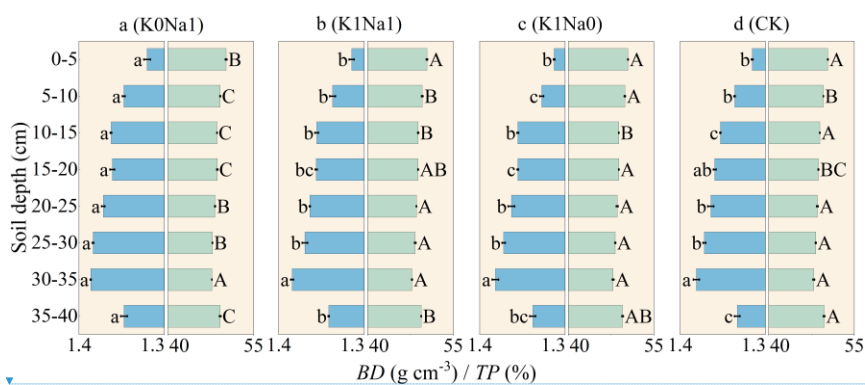
删除了: -

删除了: -

删除了: -

删除了: -

删除了: -



删除了:

374 $BD (g\ cm^{-3}) / TP (\%)$

375 Fig. 6. Soil bulk density (BD) and total porosity (TP) throughout the soil column profile
 376 under different treatments. K0Na1, K1Na1 and K1Na0 indicate the saline water at EC
 377 of $4\ dS\ m^{-1}$ with K^+/Na^+ of 0:1, 1:1 and 1:0, respectively; CK, deionized water; The
 378 blue horizon columns represent BD , while the green horizon columns represent TP ;
 379 Different lowercase letters followed means of BD indicate statistical differences ($P <$
 380 0.05) among treatments based on LSD, and different uppercase letters followed means
 381 of TP indicate statistical differences ($P < 0.05$) among treatments based on LSD. Bars
 382 indicate standard deviations of means.

删除了: capital

383 3.6 Proportion of micropores and proportion of macropores

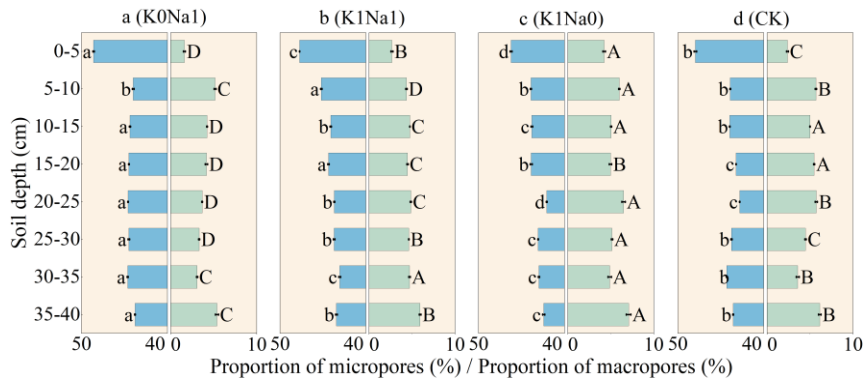
384 Micropores were the dominant pores for all treatments, the proportion of
 385 micropores accounting for more than 40% of the total soil volume, however, the
 386 proportion of macropores did not exceed 8% (Fig. 7). The 0-5 cm soil layer had the
 387 lowest proportion of macropores and retained the largest proportion of micropores
 388 compared with other depths. K0Na1 had the highest proportion of micropores and the

删除了: made up no more than

删除了: -

393 lowest proportion of macropores. K1Na0 had a greater proportion of macropores in the
 394 soil column than CK.

删除了: compared with



395
 396 Fig. 7. Proportion of micropores and proportion of macropores in total soil volume
 397 throughout the soil column profile under different treatments. K0Na1, K1Na1 and
 398 K1Na0 indicate the saline water at EC of 4 dS m⁻¹ with K⁺/Na⁺ of 0:1, 1:1 and 1:0,
 399 respectively; CK, deionized water; The blue horizon columns represent proportion of
 400 micropores, while the green horizon columns represent proportion of macropores;
 401 Different lowercase letters followed means of proportion of micropores indicate
 402 statistical differences ($P < 0.05$) among treatments based on LSD, and different
 403 uppercase letters followed means of proportion of macropores indicate statistical
 404 differences ($P < 0.05$) among treatments based on LSD. Bars indicate standard
 405 deviations of means.

删除了: capital

408 **4 Discussion**

409 **4.1 Effects of saline water on soil water movement and redistribution**

410 As a crucial soil hydraulic characteristic, K_{sat} [reflects](#) the transportation ability of
411 water and solutes (Braud et al. 2001; Maillard et al. 2011; Albalasmeh et al. 2022). The
412 cation composition and EC of soil solution affect K_{sat} by controlling electrostatic
413 repulsive pressure through surface potential and midpoint potential between adjacent
414 particles, and consequently influence water movement (Fares et al. 2000; Liu et al.,
415 2022b). Specifically, the [relative concentration of \$K^+\$ to \$Na^+\$](#) in saline water was related
416 to the swelling and dispersion of soil particles (Yu et al. 2016; Zhu et al. 2019).
417 Dispersed clay particles clogged soil macropores to subsequently restrict water
418 transport (Awedat et al., 2021). The Na^+ has a relatively higher ionicity index than K^+ ,
419 as a result, the low [relative concentration of \$K^+\$ to \$Na^+\$](#) decreased the degree of
420 covalency in clay-cation bonds, which was detrimental to clay particles aggregation
421 (Marchuk and Rengasamy 2011). Therefore, in our study, the high [relative](#)
422 [concentration of \$K^+\$ to \$Na^+\$](#) , promoted the flocculation and stabilization of soil clay
423 particles, resulting in an increased [water hydraulic conductivity \(Fig. 2\)](#).
424 After a certain period of [irrigation](#), soil moisture redistributed at different depths
425 of soil column, [\(Fig. 3\)](#). Soil water moved further down during the phase of water
426 redistribution soon after each irrigation, reducing the water content in the upper soil
427 layers. As the upper soil layers drained, the lower soil layers still had water inflow

删除了: represents

删除了: +/

删除了: ratio

删除了: K^+/Na^+ ratio

删除了: +/

删除了: ratio

删除了: infiltration rate.

删除了: water supply

删除了: .

437 (Kargas et al., 2021), increasing the water content in the lower soil layers. The results
438 also implicated that the retention of soil water by Na^+ was stronger than that by K^+ , the
439 cause may be that Na^+ can increase the thickness of the diffuse-double layers around
440 soil colloids theoretically due to its larger hydrated radius and lower charge than K^+ ,
441 and the adjacent double layers overlapped to provide more space between layers (He et
442 al., 2015), where, subsequently, more water can be retained (Fig. 3).

443 Additionally, our study showed that K1Na1 was even more beneficial than
444 deionized water for water downward transport (Fig. 3), which was due to that deionized
445 water (CK) (below 0.2 dS m^{-1}) tended to leach soluble minerals and salts, especially
446 Ca^{2+} , from the surface soil layers. This would lead to the reduction of its original solid
447 soil structural stability. In the absence of salt and Ca^{2+} , the dispersed tiny particles filled
448 the smaller pore spaces in soil, reducing even more channels for water flow and
449 exacerbating water retention in deeper soil layers (Ayers and Westcot 1985). However,
450 a lower concentration of soluble salts could increase colloid flocculation, and thereby,
451 improving soil aeration and water conductivity (Tang and She 2016).

452 4.2 Effects of saline water on soil salination and desalination process

453 Numerous factors influence soil salt leaching efficiency; for example, increasing
454 EC and reducing SAR definitely improve clay flocculation, which can enhance salt
455 leaching (Ebrahim Yahya et al., 2022). Na^+ is more likely to trigger soil clay dispersion
456 and swelling than K^+ , thus Na^+ generally inhibits water infiltration, which is detrimental

删除了: ,

删除了: He et al., 2015).

删除了: an appropriate concentration of K^+/Na^+

删除了: ,

删除了: could be because the

删除了: improve

删除了: the

删除了: of soil salts

465 to salt leaching (Smiles and Smith 2004). Adding K^+ could promote displacement of
466 the adsorbed Na^+ , and then decrease Na^+ concentration and salt accumulation in soil
467 solute through leaching.

468 A greater reduction in Na^+ concentration was associated with a higher rate of
469 cation exchange rate, and the slow rate of solute leaching from aggregates reduced the
470 total leaching efficiency (Shaygan et al., 2017). During the leaching process, water flow
471 preferentially passed through the macropores rather than aggregates. The slow water
472 transportation through aggregates induced the slow removal of solutes from the
473 aggregates, leading to a reduced leaching efficiency. In our study, the alternate leaching
474 was implemented to improve solute leaching (Figs. 4 and 5). The soil solutes diffused
475 into the aggregates surface during the rest period, improving salt leaching due to the
476 water flow in macropores (Al-Sibai et al., 1997). Saline water with more K^+ could
477 increase the magnitude of cation exchange due to the substitution of Na^+ on exchange
478 sites by K^+ with lower dispersive potential (Shaygan et al., 2017), the intensive release
479 of cations from the soil further improved salt's leaching efficiency. In addition, the
480 integrity of soil aggregates created by combining clay particles and the other soil
481 components enhanced by K^+ can benefit solute transportation (Marchuk and
482 Rengasamy 2011).

483 4.3 Effects of saline water on soil pore structure characteristics

484 The upper soil was longer exposed to water due to the long-term continuous

删除了: .

删除了: Increasing K^+/Na^+ ratio

487 irrigation, causing the particles to swell and the surface layer to loosen (Vaezi et al.
488 2017; Håkansson and Lipiec 2000), and also the decreased *BD* in the surface layer of
489 soil column (Fig. 6). The subsoil *BD* increased with depth under the impact of water
490 pressure and self-weight due to the declining pore diameter and pore branching closure
491 (Schjønning et al., 2013). And for soil at the bottom, the loss of soil particles from small
492 holes was responsible for the abrupt reduction in *BD* (Fig. 6). The value of *CROSS* in
493 saline water could reflect changes in soil *BD* and *TP*, in agreement with the result of
494 Marchuk and Marchuk (2018). The high *CROSS* implied an increase in the proportion
495 of monovalent exchangeable cations, thickening the double layer at the interface
496 between the clay surface and soil solution. Hence, soil swelling occurred at the expense
497 of water-conducting pores. Additionally, aggregates slaking and subsequent clay
498 dispersion and deposition of clay particles within the pore space contributed to the
499 reduction in *TP* (Marchuk and Marchuk 2018).

删除了:.

删除了:.

500 [Soil macropores play](#) a crucial role in water and solute transport, accounting for
501 85% of the total infiltration volume (Wilson and Luxmoore 1988; Weiler and Naef 2003;
502 Kotlar et al. 2020). [For saline water with the same EC, a decrease in \$K^+\$ concentration](#)
503 [may enhance](#) soil clay dispersion, resulting in the loosening of clay particles from the
504 aggregates. This, in turn, dispersed clay particles moved with water caused the
505 macropores to become blocked, converting them into micropores (Cameira et al., 2003),
506 thus leading to a decrease in the volume of soil macropores (Fig. 7).

删除了: Fewer soil

删除了: plays

删除了: The lower the K^+/Na^+ ratio, the more it enhanced

删除了:.

513 **5 Conclusion**

514 We explored the effects of the relative ratio of K^+ to Na^+ in saline water on soil
515 hydraulic characteristics and structural stability via a soil column experiment. Irrigation
516 with saline water of K^+/Na^+ of 1:0 caused fewer pore blockages due to soil clay particle
517 dispersion than 0:1, which increased soil saturated hydraulic conductivity. The presence
518 of K^+ accelerated the sustained Na^+ replacement and leaching, alleviating salt
519 accumulation and enhancing leaching efficiency. K^+ positively affected the
520 establishment of soil structure due to the transformation of micropores into macropores,
521 and the ever-increasing unobstructed water-conducting channels sped up water and
522 solute transport. The rational use of saline water with adequate K^+ could help mitigate
523 the structural deterioration caused by Na^+ . Appropriate adjustment of the relative
524 concentration of K^+ to Na^+ in saline water during infiltration could ameliorate soil
525 structural properties. In addition to Ca^{2+} and Mg^{2+} (primary concerns in earlier studies),
526 the relative concentration of K^+ to Na^+ is an essential indicator for assessing the
527 suitability of saline water quality for irrigation and should be considered when using
528 saline water.

529 **Author contributions**

530 Sihui Yan and Tibin Zhang conceived and designed the experiments. Sihui Yan,
531 Binbin Zhang and Tonggang Zhang led the data processing and statistical analysis,
532 Sihui Yan, Yu Cheng, Chun Wang and Min Luo performed the experiments. Sihui Yan

删除了: effect

删除了: +/

删除了: The higher

删除了: ratio

删除了: lower K^+/Na^+ ,

删除了: Increasing K^+/Na^+

删除了: K^+/Na^+

540 wrote the initial draft. Hao Feng and Kadambot H.M. Siddique contributed to review
541 and editing of the paper.

542 **Acknowledgments**

543 This work was supported by the National Key R&D Program of China (Grant No.
544 [2021YFD1900700](#)), [the Innovation Capability Support Program of Shaanxi \(Grant no.](#)
545 [2022PT-23\)](#), [the Key R&D Program of Shaan xi \(Grant no. 2023-ZDLNY-53\)](#), and
546 [China 111 project \(B12007\)](#).

删除了:) and National Natural Science Foundation

删除了: China

删除了: No. 51879224, 51509238

550 **References**

551 Albalasmeh, A., Mohawesh, O., Gharaibeh, M., Deb, S., Slaughter, L., El Hanandeh, A.: Artificial
552 neural network optimization to predict saturated hydraulic conductivity in arid and semi-arid
553 regions, *Catena*, 217, 106459, <http://dx.doi.org/10.1016/J.CATENA.2022.106459>, 2022.

删除了: <https://doi.org/10.1016/j.catena.2022.106459>,

554 Aldaz-Lusarreta, A., Giménez, R., Campo-Bescós, M.A., Arregui, L.M., Virto, I.: Effects of
555 innovative long-term soil and crop management on topsoil properties of a Mediterranean soil
556 based on detailed water retention curves, *SOIL*, 8, 655-671, [http://dx.doi.org/10.5194/SOIL-8-](http://dx.doi.org/10.5194/SOIL-8-655-2022)
557 [655-2022](http://dx.doi.org/10.5194/SOIL-8-655-2022), 2022.

删除了: <https://>

删除了: egusphere-2022-1092,

558 Al-Sibai, M., Adey, M.A., Rose, D.A.: Movement of solute through a porous medium under
559 intermittent leaching, *Eur. J. Soil Sci.*, 48, 711-725, [http://dx.doi.org/10.1046/j.1365-](http://dx.doi.org/10.1046/j.1365-2389.1997.00126.x)
560 [2389.1997.00126.x](http://dx.doi.org/10.1046/j.1365-2389.1997.00126.x), 1997.

删除了: <https://>

561 Alva, A.K., Sumner, M.E., Miller, W.P.: Relationship between ionic strength and electrical
562 conductivity for soil solutions, *Soil Sci.*, 152, 239-242, [https://doi.org/10.1097/00010694-](https://doi.org/10.1097/00010694-199110000-00001)
563 [199110000-00001](https://doi.org/10.1097/00010694-199110000-00001), 1991.

564 Aparicio, J., Tenza-Abril, A.J., Borg, M., Galea, J., Candela, L.: Agricultural irrigation of vine crops
565 from desalinated and brackish groundwater under an economic perspective. A case study in
566 Siggiewi, Malta, *Sci. Total Environ.*, 650, 734-740,
567 <https://doi.org/10.1016/j.scitotenv.2018.09.059>, 2019.

568 Awadat, A.M., Zhu, Y., Bennett, J.M., Raine, S.R.: The impact of clay dispersion and migration on
569 soil hydraulic conductivity and pore networks, *Geoderma*, 404, 115297,
570 <http://dx.doi.org/10.1016/J.GEODERMA.2021.115297>, 2021.

删除了: <https://>

删除了: j.geoderma

577 Ayers, R.S., Westcot, D.W.: Water Quality for Agriculture, FAO Irrigation and Drainage Paper 29
578 Rev 1, Rome, Italy.

579 Bao, S.D.: Soil Analysis in Agricultural Chemistry, China Agricultural Press, Beijing, China, 2005
580 (in Chinese).

581 Belkheiri, O., Mulas, M.: The effects of salt stress on growth, water relations and ion accumulation
582 in two halophyte *Atriplex* species, *Environ. Exp. Bot.*, 86, 17-28,
583 <http://dx.doi.org/10.1016/j.envexpbot.2011.07.001>, 2013.

584 Bouksila, F., Bahri, A., Berndtsson, R., Persson, M., Rozema, J., Van der Zee, S.E.A.T.M.:
585 Assessment of soil salinization risks under irrigation with brackish water in semiarid Tunisia,
586 *Environ. Exp. Bot.*, 92, 176-185, <http://dx.doi.org/10.1016/j.envexpbot.2012.06.002>, 2013.

587 Braud, I., Vich, A.I.J., Zuluaga, J., Fornero, L., Pedrani, A.: Vegetation influence on runoff and
588 sediment yield in the Andes region: observation and modelling, *J. Hydrol.*, 254, 124-144,
589 [http://dx.doi.org/10.1016/S0022-1694\(01\)00500-5](http://dx.doi.org/10.1016/S0022-1694(01)00500-5), 2001.

590 Budhathoki, S., Lamba, J., Srivastava, P., Malhotra, K., Way, T.R., Katuwal, S.: Using X-ray
591 computed tomography to quantify variability in soil macropore characteristics in pastures, *Soil
592 Tillage Res.*, 215, 105194, <http://dx.doi.org/10.1016/j.STILL.2021.105194>, 2022.

593 Buelow, M.C., Steenwerth, K., Parikh, S.J.: The effect of mineral-ion interactions on soil hydraulic
594 conductivity, *Agric. Water. Manag.*, 152, 277-285,
595 <http://dx.doi.org/10.1016/j.agwat.2015.01.015>, 2015.

596 Cameira, M.R., Fernando, R.M., Pereira, L.S.: Soil macropore dynamics affected by tillage and
597 irrigation for a silty loam alluvial soil in southern Portugal, *Soil Tillage Res.*, 70, 131-140,

删除了: https://

删除了: https://

删除了: https://

删除了: https://

删除了: j.still

删除了: https://

604 [http://dx.doi.org/10.1016/S0167-1987\(02\)00154-X](http://dx.doi.org/10.1016/S0167-1987(02)00154-X), 2003.

删除了: https://

605 Ebrahim Yahya, K., Jia, Z., Luo, W., Yuanchun, H., Ame, M.A.: Enhancing salt leaching efficiency

606 of saline-sodic coastal soil by rice straw and gypsum amendments in Jiangsu coastal area, *Ain*

607 *Shams Eng. J.*, 13, 101721, <http://dx.doi.org/10.1016/J.ASEJ.2022.101721>, 2022.

删除了: https://

608 Fares, A., Alva, A.K., Nkedi-Kizza, P., Elrashidi, M.A.: Estimation of soil hydraulic properties of a

609 sandy soil using capacitance probes and Guelph Permeameter, *Soil Sci. Soc. Am. J.*, 165, 768-

610 777, <https://doi.org/10.1097/00010694-200010000-00002>, 2000.

删除了: j.asej

611 Gharaibeh, M.A., Eltaif, N.I., Shunnar, O.F.: Leaching and reclamation of calcareous saline-sodic

612 soil by moderately saline and moderate-SAR water using gypsum and calcium chloride, *J. Plant*

613 *Nutr. Soil Sci.*, i.-Z. *Pflanzenemahr. Bodenkd.*, 172, 713-719,

614 <http://dx.doi.org/10.1002/jpln.200700327>, 2009.

615 Hack-Ten Broeke, M.J.D., Kroes, J.G., Bartholomeus, R.P., Van Dam, J.C., De Wit, A.J.W., Supit,

616 I., Walvoort, D.J.J., Van Bakel, P.J.T., Ruijtenberg, R.: Quantification of the impact of

617 hydrology on agricultural production as a result of too dry, too wet or too saline conditions,

618 *SOIL*, 2, 391-402, <http://dx.doi.org/10.5194/soil-2-391-2016>, 2016.

删除了: https://

619 Håkansson, I., Lipiec, J.: A review of the usefulness of relative bulk density values in studies of soil

620 structure and compaction, *Soil Tillage Res.*, 53, 71-85, <http://dx.doi.org/10.1016/S0167->

删除了: https://

621 1987(99)00095-1, 2000.

622 He, Y.B., Desutter, T.M., Casey, F., Clay, D., Franzen, D., Steele, D.: Field capacity water as

623 influenced by Na and EC: Implications for subsurface drainage, *Geoderma*, 245, 83-88,

624 <http://dx.doi.org/10.1016/j.geoderma.2015.01.020>, 2015.

删除了: https://

631 Hu, X., Li, Z.C., Li, X.Y., Wang, P., Zhao, Y.D., Liu, L.Y., LÜ, Y.L.: Soil macropore structure
632 characterized by X-Ray computed tomography under different land uses in the Qinghai Lake
633 watershed, Qinghai-Tibet plateau., *Pedosphere*, 28, 478-487, [http://dx.doi.org/10.1016/S1002-](http://dx.doi.org/10.1016/S1002-0160(17)60334-5)
634 0160(17)60334-5, 2018.

删除了: https://

635 Jury, W., Gardner, W.R., Gardner, W.H.: *Soil Physics*, John Wiley and Sons, New York, USA, 1991.
636 Kargas, G., Soulis, K.X., Kerkides, P.: Implications of hysteresis on the horizontal soil water
637 redistribution after infiltration, *Water*, 13, 2773-2773, <http://dx.doi.org/10.3390/W13192773>,
638 2021.

删除了: https://

639 Kim, H., Anderson, S.H., Motavalli, P.P., Gantzer, C.J.: Compaction effects on soil macropore
640 geometry and related parameters for an arable field, *Geoderma*, 160, 244-251,
641 <http://dx.doi.org/10.1016/j.geoderma.2010.09.030>, 2010.

删除了: https://

642 Kotlar, A.M., de Jong van der, Q., Andersen, H.E., Nørgaard, T., Iversen, B.V.: Quantification of
643 macropore flow in Danish soils using near-saturated hydraulic properties, *Geoderma*, 375,
644 114479, <http://dx.doi.org/10.1016/j.geoderma.2020.114479>, 2020.

删除了: https://

645 Li, Z.Y., Cao, W.G., Wang, Z.R., Li, J.C., Ren, Y.: Hydrochemical characterization and irrigation
646 suitability analysis of shallow groundwater in Hetao Irrigation District, Inner Mongolia.,
647 *Geoscience*, 36, 418-426, <https://doi.org/10.19657/j.geoscience.1000-8527.2022.012>, 2022 (in
648 Chinese).

649 Liu, B.X., Wang, S.Q., Liu, X.J., Sun, H.Y.: Evaluating soil water and salt transport in response to
650 varied rainfall events and hydrological years under brackish water irrigation in the North China
651 Plain, *Geoderma*, 422, 115954, <http://dx.doi.org/10.1016/J.GEODERMA.2022.115954>, 2022a.

删除了: https://

删除了: j.geoderma

658 Liu, X.M., Zhu, Y.C., Mclean Bennett, J., Wu, L.S., Li, H.: Effects of sodium adsorption ratio and
659 electrolyte concentration on soil saturated hydraulic conductivity, *Geoderma*, 414, 115772,
660 <http://dx.doi.org/10.1016/J.GEODERMA.2022.115772>, 2022b.

661 Luxmoore, R.J.: Micro-, meso-, and macroporosity of soils., *Soil Sci. Soc. Am. J.*, 45, 671-672,
662 <http://dx.doi.org/10.2136/sssaj1981.03615995004500030051x>, 1981.

663 Maillard, E., Payraudeau, S., Faivre, E., Grégoire, C., Gangloff, S., Imfeld, G.: Removal of pesticide
664 mixtures in a stormwater wetland collecting runoff from a vineyard catchment, *Sci. Total*
665 *Environ.*, 409, 2317-2324, <http://dx.doi.org/10.1016/j.scitotenv.2011.01.057>, 2011.

666 Marchuk, A., Marchuk, S.A., Bennett, J.A., Eyres, M.A., Scott, E.: An alternative index to ESP to
667 explain dispersion occurring in Australian soils when Na content is low, *National Soils*
668 *Conference: Proceedings of the 2014 National Soils Conference Soil Science Australia*
669 *Melbourne, Australia*, 2014.

670 Marchuk, A., Rengasamy, P.: Clay behaviour in suspension is related to the ionicity of clay-cation
671 bonds, *Appl. Clay Sci.*, 53, 754-759, <http://dx.doi.org/10.1016/j.clay.2011.05.019>.

672 Marchuk, S., Marchuk, A.: Effect of applied potassium concentration on clay dispersion, hydraulic
673 conductivity, pore structure and mineralogy of two contrasting Australian soils., *Soil Tillage*
674 *Res.*, 182, 35-44, <http://dx.doi.org/10.1016/j.still.2018.04.016>, 2018.

675 Mckenna, B.A., Kopittke, P.M., Macfarlane, D.C., Dalzell, S.A., Menzies, N.W.: Changes in soil
676 chemistry after the application of gypsum and sulfur and irrigation with coal seam water,
677 *Geoderma*, 337, 782-791, <http://dx.doi.org/10.1016/j.geoderma.2018.10.019>, 2019.

678 Prajapati, M., Shah, M., Soni, B.: A review of geothermal integrated desalination: A sustainable

删除了: https://

删除了: j.geoderma

删除了: https://

删除了: https://

删除了: https://

删除了: , 2011

删除了: https://

删除了: https://

687 solution to overcome potential freshwater shortages, *J. Clean. Prod.*, 326, 129412,
688 <http://dx.doi.org/10.1016/J.JCLEPRO.2021.129412>, 2021.

删除了: https://

删除了: j.jclepro

689 Qadir, M., Oster, J.D., Schubert, S., Noble, A.D., Sahrawat, K.L.: Phytoremediation of Sodic and
690 Saline - Sodic Soils, *Adv. Agron.*, 96, 197-247, [http://dx.doi.org/10.1016/S0065-](http://dx.doi.org/10.1016/S0065-2113(07)96006-X)
691 2113(07)96006-X, 2007.

删除了: https://

692 Qadir, M., Sposito, G., Smith, C.J., Oster, J.D.: Reassessing irrigation water quality guidelines for
693 sodicity hazard, *Agric. Water. Manag.*, 255, 107054,
694 <http://dx.doi.org/10.1016/J.AGWAT.2021.107054>, 2021.

删除了: https://

删除了: j.agwat

695 Reading, L.P., Lockington, D.A., Bristow, K.L., Baumgartl, T.: Are we getting accurate
696 measurements of Ksat for sodic clay soils? *Agric. Water. Manag.*, 158, 120-125,
697 <http://dx.doi.org/10.1016/j.agwat.2015.04.015>, 2015.

删除了: https://

698 Rengasamy, P., Marchuk, A.: Cation ratio of soil structural stability (CROSS), *Soil Res.*, 49, 280-
699 285, <http://dx.doi.org/10.1071/SR10105>, 2011.

删除了: https://

700 Sahin, U., Eroglu, S., Sahin, F.: Microbial application with gypsum increases the saturated hydraulic
701 conductivity of saline-sodic soils, *Appl. Soil Ecol.*, 48, 247-250,
702 <http://dx.doi.org/10.1016/j.apsoil.2011.04.001>, 2011.

删除了: https://

703 Schjønning, P., Lamandé, M., Berisso, F.E., Simojoki, A., Alakukku, L., Andreasen, R.R.: Gas
704 diffusion, non-darcy air permeability, and computed tomography images of a clay subsoil
705 affected by compaction, *Soil Sci. Soc. Am. J.*, 77, 1977-1990,
706 <http://dx.doi.org/10.2136/sssaj2013.06.0224>, 2013.

删除了: https://

707 Scudiero, E., Skaggs, T.H., Corwin, D.L.: Simplifying field-scale assessment of spatiotemporal

717 changes of soil salinity, *Sci. Total Environ.*, 587-588, 273-281,
718 <http://dx.doi.org/10.1016/j.scitotenv.2017.02.136>, 2017.

删除了: https://

719 Shaygan, M., Reading, L.P., Baumgartl, T.: Effect of physical amendments on salt leaching
720 characteristics for reclamation, *Geoderma*, 292, 96-110,
721 <http://dx.doi.org/10.1016/j.geoderma.2017.01.007>, 2017.

删除了: https://

722 Singh, G., Mavi, M.S., Choudhary, O.P., Gupta, N., Singh, Y.: Rice straw biochar application to soil
723 irrigated with saline water in a cotton-wheat system improves crop performance and soil
724 functionality in north-west India, *J. Environ. Manage.*, 295, 113277,
725 <http://dx.doi.org/10.1016/J.JENVMAN.2021.113277>, 2021.

删除了: https://

删除了: j.jenvman

726 Smiles, D.E., Smith, C.J.: A survey of the cation content of piggery effluents and some consequences
727 of their use to irrigate soils, *Soil Res.*, 42, 231-246, <http://dx.doi.org/10.1071/SR03059>, 2004.

删除了: https://

728 Smith, C.J., Oster, J.D., Sposito, G.: Potassium and magnesium in irrigation water quality assessment,
729 *Agric. Water. Manag.*, 157, 59-64, <http://dx.doi.org/10.1016/j.agwat.2014.09.003>, 2015.

删除了: https://

730 Sposito, G., Oster, J.D., Smith, C.J., Assouline, S.: Assessing soil permeability impacts from
731 irrigation with marginal-quality waters, *AB Reviews: Perspectives in Agriculture, Veterinary
732 Science, Nutrition and Natural Resources*. 11, 15,
733 <http://dx.doi.org/10.1079/PAVSNNR201611015>, 2016.

删除了: https://

734 Tang, S.Q., She, D.L.: Influence of water quality on soil saturated hydraulic conductivity and
735 infiltration properties, *Transactions of the Chinese Society for Agricultural Machinery*, 47, 108-
736 114, <https://doi.org/10.6041/j.issn.1000-1298.2016.10.015>, 2016 (in Chinese).

737 Tsai, W.T., Liu, S.C., Chen, H.R., Chang, Y.M., Tsai, Y.L.: Textural and chemical properties of

745 swine-manure-derived biochar pertinent to its potential use as a soil amendment, *Chemosphere*,
746 89, 198-203, <https://doi.org/10.1016/j.chemosphere.2012.05.085>, 2012.

747 Vaezi, A.R., Ahmadi, M., Cerdà, A.: Contribution of raindrop impact to the change of soil physical
748 properties and water erosion under semi-arid rainfalls, *Sci. Total Environ.*, 583, 382-392,
749 <http://dx.doi.org/10.1016/j.scitotenv.2017.01.078>, 2017.

750 Weiler, M., Naef, F.: Simulating surface and subsurface initiation of macropore flow, *J. Hydrol.*,
751 273, 139-154, [http://dx.doi.org/10.1016/S0022-1694\(02\)00361-X](http://dx.doi.org/10.1016/S0022-1694(02)00361-X), 2003.

752 Wilson, G.V., Luxmoore, R.J.: Infiltration, macroporosity, and mesoporosity distributions on two
753 forested watersheds, *Soil Sci. Soc. Am. J.*, 52, 329-335,
754 <http://dx.doi.org/10.2136/sssaj1988.03615995005200020005x>, 1988.

755 Xu, J., Huang, P.M.: *Soil Science*, China Agriculture Press, Beijing, China, 2010 (in Chinese).

756 Yang, G., Li, F., Tian, L., He, X., Gao, Y., Wang, Z., Ren, F.: Soil physicochemical properties and
757 cotton (*Gossypium hirsutum* L.) yield under brackish water mulched drip irrigation, *Soil*
758 *Tillage Res.*, 199, 104592, <https://doi.org/10.1016/j.still.2020.104592>, 2020.

759 Yin, C.Y., Zhao, J., Chen, X.B., Li, L.J., Liu, H., Hu, Q.L.: Desalination characteristics and
760 efficiency of high saline soil leached by brackish water and Yellow River water, *Agric. Water*
761 *Manag.*, 263, 107461, <http://dx.doi.org/10.1016/J.AGWAT.2022.107461>, 2022.

762 Yu, Z.H., Liu, X.M., Xu, C.Y., Xiong, H.L., Li, H.: Specific ion effects on soil water movement,
763 *Soil Tillage Res.*, 161, 63-70, <http://dx.doi.org/10.1016/j.still.2016.03.004>, 2016.

764 Zhang, H.X., Xie, Y.Z.: Alleviating freshwater shortages with combined desert-based large-scale
765 renewable energy and coastal desalination plants supported by Global Energy Interconnection,

删除了: https://

删除了: https://

删除了: https://

删除了: https://

删除了: j.agwat

删除了: https://

772 Glob. Energy Interconnec., 2, 205-213, <http://dx.doi.org/10.1016/j.gloi.2019.07.013>, 2019.

删除了: https://

773 Zhang, T.B., Zhan, X.Y., He, J.Q., Feng, H., Kang, Y.H.: Salt characteristics and soluble cations
774 redistribution in an impermeable calcareous saline-sodic soil reclaimed with an improved drip
775 irrigation, Agric. Water. Manag., 197, 91-99, <https://doi.org/10.1016/j.agwat.2017.11.020>,
776 2018.

777 Zhu, Y., Bennett, J.M., Marchuk, A.: Reduction of hydraulic conductivity and loss of organic carbon
778 in non-dispersive soils of different clay mineralogy is related to magnesium induced
779 disaggregation, Geoderma, 349, 1-10, <https://doi.org/10.1016/j.agwat.2017.11.020>, 2019.

删除了: <https://doi.org/10.1016/j.geoderma.2019.04.019>,
2019.